Femtosecond Electronic Heat-Transport Dynamics in Thin Gold Films

S. D. Brorson, J. G. Fujimoto, and E. P. Ippen
Department of Electrical Engineering and Computer Science and Research Laboratory of Electronics, Massachusetts Institute of Technology, Cambridge, Massacusetts 02139
(Received 7 August 1987)

We have observed ultrafast heat transport in thin gold films under femtosecond laser irradiation. Time-of-flight (front-pump back-probe) measurements indicate that the heat transit time scales linearly with the sample thickness, and that heat transport is very rapid, occurring at a velocity close to the Fermi velocity of electrons in Au.

PACS numbers: 72.15.Cz, 72.15.Lh, 73.50.Gr, 73.60.Aq

Recently, the ultrafast dynamics of hot electrons in metals has become an area of active investigation. Early theoretical predictions[1] showed that under ultrafast excitation conditions the electrons in a metal can exist out of equilibrium with the lattice for times less than the electron energy relaxation time. After excitation, the electrons relax to equilibrium with the lattice by the emission of phonons. This phenomenon has been observed experimentally by transient thermomodulation[2-4] and femtosecond photoemission.[5] Unresolved, however, is the role of heat transport in the dynamics of the hot-electron–lattice system. This is because most experiments performed to date cannot distinguish between relaxation due to heat flow out of the probed region and electronic relaxation via phonon emission. Here we present the results of both front-probe and back-probe thermomodulation measurements designed to separate these effects. Using films of varying thickness, we are able to determine the heat transit time through the sample as a function of sample thickness. We find that heat transport occurs at the Fermi velocity, v_F.

Our experiment exploits the reflectivity changes induced by electronic temperature changes in a metal film.[2,4,6] An ultrashort laser pulse heats the electrons at the front surface of a noble metal (Au). This changes the occupancy of electronic states near the Fermi level. Since there is an allowed transition from the d band to states near the Fermi level at our laser wavelength ($\lambda_0 = 630$ nm), changes in the electronic occupancy near E_F affect this transition rate. The imaginary part of the dielectric function $\epsilon = \epsilon_1 + i\epsilon_2$ is sensitive to changes in the transition rate. Thus, since the sample reflectivity R depends upon ϵ, the experimental signature is a change in R as the electron temperature changes. Although other effects can also cause temperature-dependent reflectivity changes, they are not significant on a femtosecond time scale.[4] Measurement of the reflectivity with a delayed probe pulse monitors the surface electronic temperature as a function of time. In our experiment, we pump the front surface of the sample and probe the reflectivity change at either the back or front surface (Fig. 1). The probe of the back-surface reflectivity allows us to measure the heat transit time, while the probing of the front monitors the reflectivity transient decay due to both heat transport and energy relaxation. The two measurements are complementary, and yield additional information about the electronic dynamics when taken together.

The experiments were performed on films of gold deposited on sapphire. Sample thicknesses ranged from 200 to 3000 Å. All samples used were thicker than the optical skin depth ($\simeq 150$ Å). The thickness of the films was monitored during deposition and was also measured with a Daktek film-thickness instrument. Our laser source was a colliding-pulse mode-locked (CPM) dye laser employing four prisms to control the cavity dispersion. $\lambda_0 = 630$ nm, $t_p = 96$ fs FWHM (sech^2) for all results shown here. Typically, the average output power of the CPM laser is about 10 mW, and the pulse repetition rate is 100 MHz. The pump and probe beams were derived from a conventional pump/probe setup. A motor-driven stepper stage with 0.1-μm resolution was employed to vary the delay between the pump and probe pulses. For the back-probe experiment, the pump beam was chopped and focused onto the front surface of the

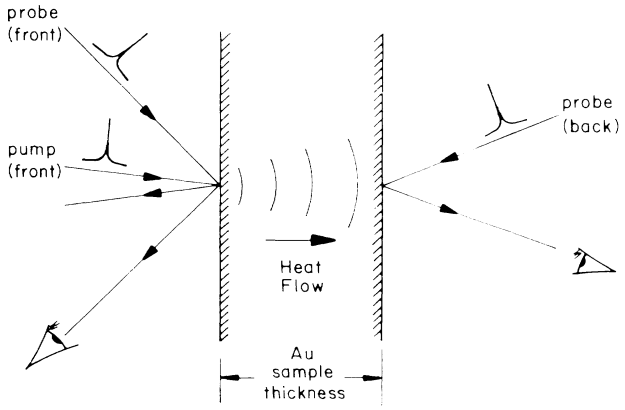

FIG. 1. Schematic of the experimental setup. The sample is pumped on the front surface, and the change in reflectivity at either the front or the back surface is probed.

sample with a 40× microscope objective, while the probe was similarly focused onto the back of the sample. The focal-spot diameter was measured with a pinhole to be ≤ 2 μm, giving an energy fluence of $\simeq 1$ mJ/cm^2 at the focus. The reflected probe beam was monitored with a photodiode. The thermomodulation signal was detected with a lock-in amplifier tuned to the chopping frequency of the pump. The zero-delay point was determined by reversing the role of pump and probe beams and repeating the experiment. In the case of the front-probe experiment, the pump was chopped, both beams were focused through a 40× microscope objective, and the reflected probe was monitored as described above.[2,4]

Shown in Fig. 2 are back-probe data for films 500, 1000, 2000, and 3000 Å thick. (It was not possible to study samples thinner than 500 Å with use of the back-probe technique because of interference due to pump-beam leakage through the metal.) The sign of $\Delta R/R$ is negative, since smearing the occupancy of states at the Fermi level causes an increase in absorption at our wavelength. Note that the delay time of the rise of the reflectivity change increases with sample thickness. This is a direct consequence of the finite time needed for heat to propagate through the sample. Note, furthermore, that the measured delay is very short, i.e., it takes only ≈ 100 fs for heat to travel 1000 Å. Another interesting feature is that the rise time of the signal increases slightly with increasing thickness. This indicates spreading in the front edge of the electron-velocity distribution which propagates through the sample. At present, the origin of this phenomenon is unknown, although it may be related to small-angle scattering.

The experiment was repeated several times for different film thicknesses. Numerical fits were performed on each trace to determine the rising-edge delay as a function of sample thickness. These results are summarized in Fig. 3. Several features are noteworthy. First, the measured delays are much shorter than would be expected if the heat were carried by the diffusion of electrons in equilibrium with the lattice (tens of picoseconds). This suggests that heat is transported via the electron gas alone, and that the electrons are out of equilibrium with the lattice on this time scale. Second, since the delay increases approximately linearly with the sample thickness (see Fig. 3), we may extract a heat-transport velocity of $\simeq 10^8$ cm/s. This is of the same order of magnitude as the Fermi velocity of electrons in Au, 1.4×10^8 cm/s. Finally, a best-fit straight line drawn through the data in Fig. 3 and extrapolated back to $t=0$ intersects the L axis at $L=290$ Å. This is reasonable, since this is roughly twice the skin depth of the metal.

The magnitude of the observed reflectivity change was monitored at the lock-in amplifier. The normalized modulation $\Delta R/R$ was on the order of 1×10^{-5} for 500-Å films, and decreased slowly to $\simeq 3\times 10^{-6}$ for Au film thickness L of 2000 Å. It was not possible to determine the functional dependence of $\Delta R/R$ on L since the sample-to-sample variations of $\Delta R/R$ were quite large. We performed these experiments using laser intensities varying over a factor of 10 on the 500-Å, and over a factor of 2 on the 1000-Å sample. We found that the delay, as well as the shape of each trace, was not affected by intensity changes. The modulation $\Delta R/R$ was observed to vary linearly with the intensity of the pump laser for all film thicknesses.

The effects of ultrafast heat transport are also observed in the results of front-probe experiments when the sample thickness is varied. Figure 4 shows reflectivity-

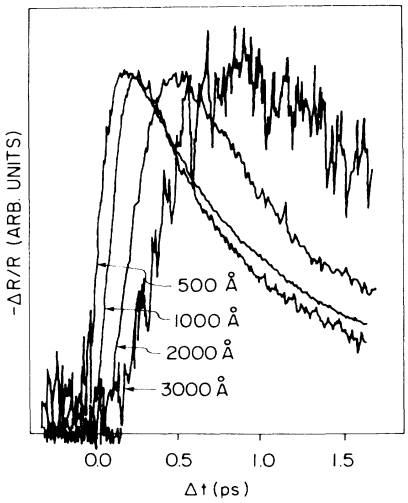

FIG. 2. Rear-surface-probe data for Au films 500, 1000, 2000, and 3000 Å thick. The delay of the rising edge is determined by the heat-transport time. The zero-delay position is determined by reversing the roles of the pump and probe beams, as described in the text.

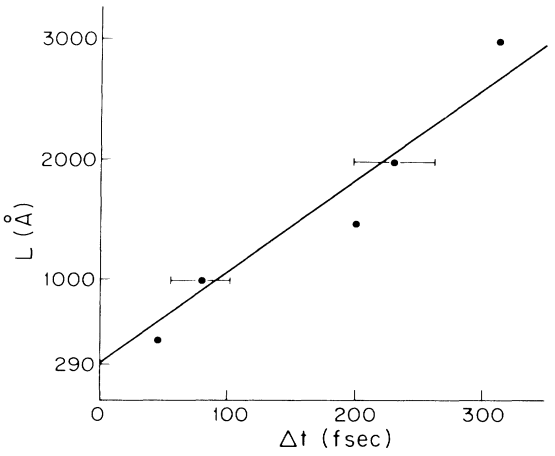

FIG. 3. Sample thickness vs time of flight for various Au films 500, 1000, 1500, 2000, and 3000 Å thick. Note that the delay scales linearly with the sample thickness. Fitting a least-squares line to the data points yields an L-axis intercept of $L=290$ Å at $t=0$.

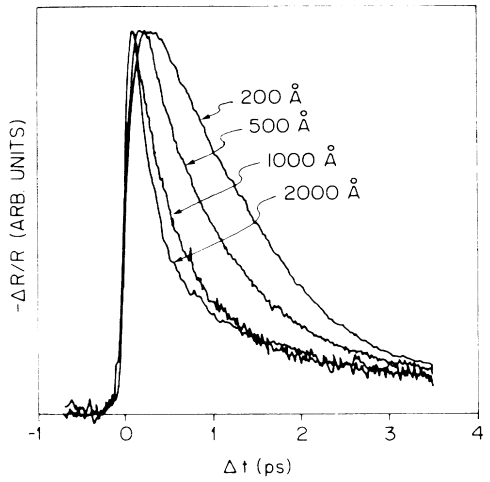

FIG. 4. Front-surface-probe data for Au films 200, 500, 1000, and 2000 Å thick. As can be seen, the reflectivity-decay time decreases as the sample thickness increases, up to samples $\simeq 1000$ Å thick. This supports the conclusion that the heat-transport mechanism is very fast.

decay data for gold films 200, 500, 1000, and 2000 Å thick. As can be seen, increasing L decreases the observed reflectivity-decay time constant. This can be understood in the following way. When the sample thickness is long compared to the optical skin depth ($L \gg d_0$, where $d_0 \approx 150$ Å), transport and energy relaxation occur simultaneously. In this case, the observed reflectivity decay is very fast since two competing processes remove energy from the probed region of the sample. Conversely, when the sample length decreases to the order of the optical skin depth ($L \approx d_0$), less transport occurs, and the reflectivity decay is primarily due to energy relaxation. The net result is that as the sample dimensions decrease, the front-surface reflectivity-decay time increases.

The magnitude of $\Delta R/R$ at the front surface was $\simeq 3\times 10^{-4}$ for samples with $L = 200$ Å. $\Delta R/R$ dropped to 2×10^{-5} for $L = 500$ Å, and then decreased more slowly as L increased. Presently, it is unclear why $\Delta R/R$ changes so dramatically for thin samples, although it is well known[7] that the optical properties of very thin (< 300 Å) Au samples can differ from bulk values. For a given L, varying the laser intensity over 1 order of magnitude did not affect the shape of the front-probe curves for $L > 500$ Å, and $\Delta R/R$ varied linearly with pump intensity.

Since the heat moves at a velocity comparable to v_F, it is natural to question exactly how the transport takes place. Recall that the motion of an individual transport electron is a random walk. Since those electrons which lie close to the Fermi surface are the principal contributors to transport, the heat-carrying electrons move at v_F. In the limit of lengths longer than the momentum relaxation length, l_p, the random-walk behavior is averaged, and the electron motion is subject to a diffusion equation. Conversely, on a length scale shorter than l_p the electrons move ballistically with a velocity close to v_F. In our experiments, it is not clear which effect (if either) will dominate the transport process. We shall treat each limiting case in turn.

In the diffusion limit, it is assumed that the electronic and lattice systems are in local equilibrium with themselves, and can hence be described as a coupled, two-temperature system. The space and time evolution of the electron and lattice temperatures (T_e and T_l, respectively) is governed by a pair of coupled nonlinear diffusion equations,[8]

$$C_e(T_e)\partial T_e/\partial t = K\nabla^2 T_e - g(T_e - T_l) + A(z,t), \quad (1a)$$

$$C_l \partial T_l/\partial t = g(T_e - T_l). \quad (1b)$$

Equation (1a) describes the evolution of the electron temperature under diffusion, coupling to the lattice, and laser irradiation. (1b) describes the lattice temperature dynamics. Here $A(z,t)$ is the space- and time-dependent energy source (i.e., the laser pulse), C_e and C_l are the electronic and lattice heat capacities, respectively, K is the electronic thermal conductivity, and g is the electron-phonon coupling constant. No diffusion term appears in (1b) since heat diffuses much more rapidly through the electron gas than through the lattice.

In the uncoupled limit ($g = 0$) for small changes in electron temperature, the electronic heat capacity may be approximated as constant and Eq. (1a) reduces to the diffusion equation. In this case, the distance traveled by the heat varies with the square root of time [$L = (D\Delta t)^{1/2}$, where $D = K/C_e$ is thermal diffusivity]. Choosing reasonable values for the diffusion parameters ($K = 3.1$ W/cm K, and $C_e = 1.84\times 10^{-2}$ J/cm^3 K at $t_e = 300$ K), we find that heat propagates only 100 Å after 100 fs, which is ten times slower than observed. However, when both heat transport and electron cooling occur simultaneously, the behavior is more complex. The cooling of the electron temperature to the lattice can make the heat transit time deviate from the expected $\Delta t \simeq L^2$ behavior and assume quasilinear behavior with $L/\Delta t \approx v_F$ over some range of sample dimensions. Thus it is difficult to distinguish between diffusive and ballistic behavior on the basis of transit-time measurements. For higher temperature changes, the relationship between Δt and L is further complicated by the fact that the diffusivity D is a function of electron temperature.

For length scales shorter than the momentum relaxation length, the electron motion is ballistic. In this situation, hot electrons are created at the front of the sample by the pump pulse. These electrons propagate through the sample without experiencing any large-angle scattering and are detected at the rear surface after a delay $\Delta t = L/v_F$. The importance of this effect may be appreci-

ated by consideration of the different hot-electron scattering lengths reported in the literature. The electron-electron scattering length in Au, l_{ee}, has been calculated by Krolikowski and Spicer from the optical density of states deduced from photoemission.[9] They find that $l_{ee} \propto (E - E_F)^{-2}$ for electrons close to the Fermi level. For 2-eV electrons, $l_{ee} \approx 350$ Å, increasing to 800 Å for 1-eV electrons. The electron-phonon scattering length, l_{ep}, is usually inferred from conductivity data. Using Drude relaxation times,[10] we compute $l_{ep} \approx 420$ Å at 273 K. This is shorter than l_{ee}, but of the same order of magnitude. Thus we would expect that both electron-electron and electron-phonon scattering are important on this length scale. However, since conductivity experiments are steady-state measurements, the contribution of phonon scattering in a femtosecond-regime experiment, such as ours, is uncertain.

On the experimental side, internal photoemission measurements of $\simeq$1-eV hot electrons generated in Au yield "attenuation lengths," l_a, of 700 Å[11] or 740 Å.[12,13] Although l_a is not equivalent to the momentum-relaxation length, it does indicate the distance over which large-angle scattering becomes important.[14] Also, l_a is indicative of the combined effects of electron-electron and electron-phonon scattering[11] which determine the heat-transport behavior in our experiment.

Since our sample dimensions are not much larger than both theoretically predicted and experimentally measured momentum- and energy-relaxation lengths, ballistic motion can be assumed to play a role in the transport we observe. This is consistent with our observation that the heat transit time does not change with laser intensity over the range of our experiment. In ballistic transport, changing the pump intensity only changes the number of electrons which participate in the transport process; the actual transport dynamics remains unaffected.

In summary, we have measured the dynamics of ultrafast heat transport in thin Au films by transient thermomodulation. Our results indicate that heat is carried by nonequilibrium electrons. Heat transport occurs on a femtosecond time scale, with a delay which scales approximately linearly with thickness. Using both front-probe and back-probe techniques, we observe a heat-transport velocity of the same order as v_F. Simple scattering arguments suggest that ballistic electronic motion may contribute to heat transport in the time and length regime under study.

The authors would like to acknowledge helpful discussion with R. W. Schoenlein, G. L. Eesley, and C. A. Paddock. One of us (S.D.B.) acknowledges with pleasure the support of a doctoral fellowship granted by the IBM Corporation. Another (J.G.F.) acknowledges support from the National Science Foundation Presidential Young Investigators Program Contract No. 8552701-ECS. This work was supported in part by the U.S. Air Force Office of Scientific Research through Grant No. 85-0213 and the Joint Services Electronics Program under Contract No. DAAL03-86-K-0002.

[1]M. I. Kaganov, I. M. Lifshitz, and L. V. Tanatarov, Zh. Eksp. Teor. Fiz. **31**, 232 (1956) [Sov. Phys. JETP **4**, 173 (1957)].

[2]G. L. Eesley, Phys. Rev. Lett. **51**, 2140 (1983).

[3]H. E. Elsayed-Ali, T. B. Norris, M. A. Pessot, and G. A. Mourou, Phys. Rev. Lett. **58**, 1212 (1987).

[4]R. W. Schoenlein, W. Z. Lin, J. G. Fujimoto, and G. L. Eesley, Phys. Rev. Lett. **58**, 1680 (1987).

[5]J. G. Fujimoto, J. M. Liu, E. P. Ippen, and N. Bloembergen, Phys. Rev. Lett. **53**, 1837 (1984).

[6]G. L. Eesley, Phys. Rev. B **33**, 2144 (1986).

[7]P. B. Johnson and R. W. Christy, Phys. Rev. B **6**, 4370 (1972).

[8]S. I. Anisimov, B. L. Kapeliovich, and T. L. Perelman, Zh. Eksp. Teor. Fiz. **66**, 776 (1974) [Sov. Phys. JETP **39**, 375 (1975)].

[9]W. F. Krolikowski and W. E. Spicer, Phys. Rev. B **1**, 478 (1970).

[10]The relevant parameters were culled from N. W. Ashcroft and N. D. Mermin, *Solid State Physics* (Holt, Reinhart, and Winston, New York), 1976).

[11]S. M. Sze, J. L. Moll, and T. Sugano, Solid State Electron. **7**, 509 (1964).

[12]W. G. Spitzer, C. R. Crowell, and M. M. Atalla, Phys. Rev. Lett. **8**, 57 (1962).

[13]C. R. Crowell, W. G. Spitzer, L. E. Howarth, and E. E. LaBate, Phys. Rev. **127**, 2006 (1962).

[14]C. R. Crowell and S. M. Sze, in *Physics of Thin Films,* edited by G. Hass and R. E. Thun (Academic, New York, 1967), Vol. 4.